

To cite this article: WANG H L, YIN C Y, LU L Y, et al. Cooperative path following control of UAV and USV cluster for maritime search and rescue[J/OL]. Chinese Journal of Ship Research, 2022, 17(5). <http://www.ship-research.com/en/article/doi/10.19693/j.issn.1673-3185.02916>.

DOI: 10.19693/j.issn.1673-3185.02916

Cooperative path following control of UAV and USV cluster for maritime search and rescue



WANG Haoliang¹, YIN Chenyang¹, LU Liyu¹, WANG Dan², PENG Zhouhua^{*2}

¹ College of Marine Engineering, Dalian Maritime University, Dalian 116026, China

² College of Marine Electrical Engineering, Dalian Maritime University, Dalian 116026, China

Abstract: [Objectives] This paper studies a three-dimensional (3D) cooperative path-following control problem in the process of maritime search and rescue for a heterogeneous unmanned cluster system composed of unmanned aerial vehicles (UAVs) and unmanned surface vehicles (USVs). [Methods] First, kinematic models of the UAVs and USVs are established under a fixed coordinate system and body coordinate system. In order to design a 3D path-following controller suitable for motion control, an air coordinate system is established, and the path tracking error models of the UAVs and USVs are established in the Serret-Frenet coordinate system. Next, a 3D line-of-sight (LOS) guidance law is designed at the kinematic level, and a cooperative path-following control method suitable for heterogeneous clusters of marine vehicles is proposed, allowing the UAVs and USVs to track the preset parameterized path. Finally, the stability of the control system is analyzed based on the Lyapunov stability theory. [Results] The simulation results verify the effectiveness of the proposed cooperative path-following control method for heterogeneous clusters of marine vehicles. [Conclusions] The results of this study can provide references for maritime search and rescue by using the proposed cooperative path-following control method.

Key words: maritime search and rescue; unmanned aerial vehicle (UAV); unmanned surface vehicle (USV); 3D LOS guidance law; cooperative path following

CLC number: U674.91

0 Introduction

As the main means of international freight transport, marine transport accounts for more than 90% of the annual international trade freight volume. Due to the complex and changeable marine environment, maritime accidents caused by natural and human factors often occur during shipping^[1]. Accord-

ing to data released by the China Maritime Search and Rescue Center, 1 527 search and rescue operations were organized from July 2021 to March 2022. For those operations, 9 138 search and rescue ships and 235 search and rescue aircraft were dispatched, ultimately searching and rescuing 1 054 ships and 9 122 people in distress. The number of people successfully rescued was 8 703. Clearly, the

Received: 2022 - 05 - 18

Accepted: 2022 - 09 - 04

Supported by: National Natural Science Foundation of China (51979020, 51909021, 51939001, 52071044); National Youth Top Talent Program (36261402); National Key Research and Development Program of China (2016YFC0301500); Basic Research Project of Higher Education Institutes of Liaoning Province (LJKZ0044, LJKQZ2021007); Xingliao Talents Program of Liaoning Province (XLYC2007188); High-level Talent Innovation Support Program of Dalian Science and Technology Bureau (2020RQ013); Fundamental Research Funds for the Central Universities (31320211345, 3132021109)

Authors: WANG Haoliang, male, born in 1985, Ph.D., associate professor, master supervisor. Research interests: path planning and cooperative control of underwater unmanned vehicles. E-mail: haoliang.wang12@dmlu.edu.cn

WANG Dan, male, born in 1960, Ph.D., professor, doctoral supervisor. Research interests: multi-agent systems and their applications in ocean vehicles. E-mail: dwang@dmlu.edu.cn

PENG Zhouhua, male, born in 1982, Ph.D., professor, doctoral supervisor. Research interests: ocean vehicle guidance and control, unmanned vessel cluster control. E-mail: zhpeng@dmlu.edu.cn

***Corresponding author:** PENG Zhouhua

rapid development of the shipping industry is inevitably accompanied by frequent maritime accidents. Therefore, further improving China's maritime search and rescue capabilities is of great significance.

At present, most maritime search and rescue operations require manual participation, and the efficiency of search and rescue is relatively low^[2]. Amid the development of intelligent equipment, the application of heterogeneous unmanned systems in maritime search and rescue has been widely concerned. Compared with the traditional maritime search and rescue methods, unmanned systems can effectively reduce the operation cost and locate the maritime search and rescue target quickly and accurately. As an important tool for maritime search and rescue, unmanned surface vehicles (USVs) can search and rescue for a long time in a wide range under complex and dangerous sea conditions. However, USVs cannot obtain search and rescue information quickly and accurately due to their limited visual field information. Unmanned aerial vehicles (UAVs) can make up for the limitation of the USVs' visual field with their advantages of 3D maneuverability and wide visual field. USVs can also solve UAVs' problems of short duration and small payload capacity^[3]. In the process of maritime search and rescue, UAVs can transmit information about the accident site over a long distance by the on-board high-definition cameras and long-distance video transmission equipment. Reciprocally, UAVs can provide data relay and power supply services for UAVs to ensure that information can be effectively transmitted back. In this way, the command department can understand the accident situation and deploy rescue measures timely, thereby effectively improving the efficiency and success rate of search and rescue. In addition, when ships transporting dangerous and toxic goods have an accident, unmanned cluster systems can effectively prevent contact and inhalation poisoning and other accidents from happening to search and rescue personnel. For the above reasons, this paper intends to use a heterogeneous unmanned cluster system composed of UAVs and USVs for maritime search and rescue and discuss the cooperative path-following control technology used in the search and rescue process.

Regarding the research on the path-following control of USVs, Liu et al.^[4] proposed a path-following control method based on line-of-sight-extended state observer-model predictive control,

ultimately solving the path-following control problem of USVs under the influence of water flow disturbance. Luan et al.^[5] designed the path-following control rate by introducing the Serret-Frenet coordinate system, referring to the position of USVs, and employing the Lyapunov direct method. In this way, they solved the path-following control problem of USVs under the conditions of external disturbance and model uncertainty. Yu et al.^[6] proposed a backstepping adaptive path-following control method for USVs based on surge-varying line-of-sight (LOS) guidance, which solved the path-following problem of USVs in the cases of mixed uncertainties in the model and saturation of controller input. Gu et al.^[7] proposed an anti-interference cooperative path-following controller under the condition of considering model uncertainty and environmental interference and thereby solved the cooperative path-following control problem of multiple USVs in directional communication topology. Liu et al.^[8] proposed a path-following control method based on the backstepping technique and LOS guidance. In this way, they solved the cooperative path-following problem of multiple USVs on a closed path curve and ultimately achieved a symmetric formation mode. Gu et al.^[9] proved that the LOS guidance method had the advantages of simplicity, high efficiency, strong anti-interference ability, and easy implementation by comparing three path-following guidance methods: pure-pursuit guidance, parallel approach guidance, and LOS guidance. Moreover, they also analyzed the future development orientation of LOS guidance.

Concerning the research on the path-following control of UAVs, Zhang et al.^[10] proposed an on-line reconfigurable LOS control method that could effectively compensate for the steady-state error and sideslip angle caused by wind during the path-following control of UAVs. Ghommam et al.^[11] used the kinematic model of UAVs to comparatively analyze the carrot path-following algorithm and pure-pursuit LOS guidance and verified the effectiveness of the two algorithms, respectively. Jin et al.^[12] proposed a method combining the backstepping method and LOS with fixed convergence time for the time-fixed path-following control of UAVs in the cases of external interference and actuator failure. Cui et al.^[13] proposed a 3D path-following algorithm based on the vector field method, achieving the 3D path-following of fixed-wing UAVs. Yan et al.^[14] solved the path-following control problem

of multiple UAVs by introducing the Serret-Frenet coordinate system and adjusting the speed of UAVs to synchronize the positions of the corresponding UAVs. Liu et al. [15] proposed a path-following controller based on the backstepping method to solve the cooperative path-following control problem of multiple UAVs in a 3D space.

Although various methods have been used to study the path-following control of UAVs in the above literature, the main research object is a single UAV[4-6,10-13]. For cooperative cluster control [7-9, 14-15], most studies are limited to homogeneous vehicles, and little research has been carried out on heterogeneous unmanned cluster systems. Therefore, drawing on the above research results, this paper intends to investigate the cooperative maritime search and rescue operations of heterogeneous cluster systems composed of USVs and UAVs. Compared with the existing research results on the path-following control of unmanned vehicles, the proposed 3D path-following controller for heterogeneous unmanned cluster systems for maritime search and rescue has the following advantages. 1) Different from path-following control that only considers a single unmanned vehicle or cooperative path-following controllers considering a two-dimensional (2D) horizontal/vertical plane, this paper solves the cooperative path-following control problem of multiple unmanned vehicles at the three-dimensional (3D) level. 2) Different from the cooperative path-following control only taking into account homogeneous unmanned vehicles, this paper solves the cooperative path-following control problem of heterogeneous unmanned cluster systems composed of UAVs and USVs.

Specifically, the kinematic models of USVs and UAVs were constructed in this paper. Subsequently, the guidance velocity, guidance angle, and guidance angular velocity of USVs and UAVs were designed at the kinematic level so that the UAVs and USVs could follow the given parameterized path and keep the path parameters consistent. Then, the motion control laws of USVs and UAVs were designed on the basis of LOS guidance, and the stability of the control system was analyzed under the Lyapunov stability theory. Finally, the effectiveness of the proposed collaborative path-following control method for heterogeneous unmanned cluster systems for maritime search and rescue was verified by simulation analysis.

1 Model of UAVs and USVs

1.1 Basic coordinate systems

To more clearly express the motion law of the vehicles, this paper built a fixed coordinate system $O_E X_E Y_E Z_E$ and a vehicle body coordinate system $O_{ib} X_{ib} Y_{ib} Z_{ib}$ (Fig. 1) to describe the motion states of the vehicles. A random point in the sea was taken as the origin O_E of the fixed coordinate system $\{I\}$; the north of the earth was taken as the positive direction of the X_E axis; the east of the earth was adopted as the positive direction of the Y_E axis; the Z_E axis pointed to the center of the earth along the plumb line. Moreover, the center of mass of the i -th vehicle ($i = 1, 2, \dots, N$, where N was the total number of vehicles) was taken as the origin O_{ib} of the vehicle body coordinate system $\{B_i\}$; the advance direction of the vehicle was defined as the positive direction of the X_{ib} axis; the positive direction of the Z_{ib} axis was perpendicular to the plane of the vehicle and pointed down; according to the right-hand rule, the Y_{ib} axis was perpendicular to the X_{ib} axis and its positive direction was the one pointing to the right side of the vehicle body.

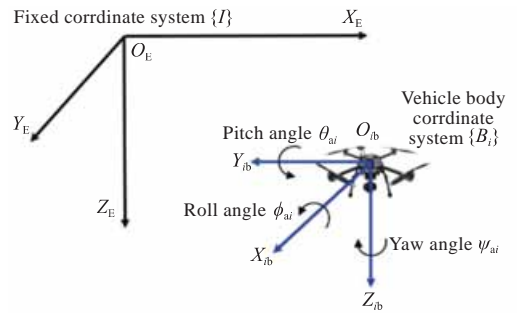


Fig. 1 Fixed coordinate system and vehicle body coordinate system

1.2 Kinematic models of UAVs and USVs

Regarding the unmanned formation system composed of N UAVs and USVs, the number of USVs was set to $1-M$, and that of UAVs was set to $M+1-N$. According to Refs. [16-17], the kinematic model of the i -th USV in a formation system composed of M USVs is as follows

$$\begin{cases} \dot{x}_{si} = u_{si} \cos \psi_{si} - v_{si} \sin \psi_{si} \\ \dot{y}_{si} = u_{si} \sin \psi_{si} + v_{si} \cos \psi_{si} \\ \dot{\psi}_{si} = r_{si} \end{cases} \quad (1)$$

where x_{si} and y_{si} are the positions of the USV in the fixed coordinate system $\{I\}$; u_{si} and v_{si} are the velocities of the USV along the X_{ib} axis and the Y_{ib} axis, respectively; ψ_{si} is the yaw angle of the USV; r_{si} is

the yaw angular velocity of the USV.

Regarding the quadrotor UAV that was adopted as the research object of this paper, Ref. [18] revealed that such a UAV controlled its motion in six degrees of freedom in space by the lift/drag force generated by rotor rotation and the velocity differences among the rotors. The kinematic model of the i -th UAV in the formation system composed of $N - M$ UAVs is as follows [19]

$$\begin{cases} \dot{x}_{ai} = u_{ai} \cos \psi_{ai} \cos \theta_{ai} + v_{ai} (\cos \psi_{ai} \sin \theta_{ai} \sin \phi_{ai} - \sin \psi_{ai} \sin \phi_{ai}) + w_{ai} (\sin \psi_{ai} \sin \phi_{ai} + \cos \psi_{ai} \sin \theta_{ai} \cos \phi_{ai}) \\ \dot{y}_{ai} = u_{ai} \sin \psi_{ai} \cos \theta_{ai} + v_{ai} (\cos \psi_{ai} \cos \phi_{ai} + \sin \psi_{ai} \sin \theta_{ai} \sin \phi_{ai}) + w_{ai} (\sin \psi_{ai} \sin \theta_{ai} \cos \phi_{ai} - \cos \psi_{ai} \sin \phi_{ai}) \\ \dot{z}_{ai} = -u_{ai} \sin \theta_{ai} + v_{ai} \cos \theta_{ai} \sin \phi_{ai} + w_{ai} \cos \theta_{ai} \cos \phi_{ai} \\ \dot{\phi}_{ai} = (p_{ai} \cos \theta_{ai} + q_{ai} \sin \phi_{ai} \sin \theta_{ai} + r_{ai} \cos \phi_{ai} \sin \theta_{ai}) / \cos \theta_{ai} \\ \dot{\theta}_{ai} = q_{ai} \cos \phi_{ai} + r_{ai} \sin \phi_{ai} \\ \dot{\psi}_{ai} = (q_{ai} \sin \phi_{ai} + r_{ai} \cos \phi_{ai}) / \cos \theta_{ai} \end{cases} \quad (2)$$

where x_{ai} , y_{ai} , and z_{ai} are the positions of the UAV in the fixed coordinate system $\{I\}$; u_{ai} , v_{ai} , and w_{ai} are the velocities of the UAV along the X_{ib} , Y_{ib} , and Z_{ib} axes, respectively; ϕ_{ai} , θ_{ai} , and ψ_{ai} are the roll angle, pitch angle, and yaw angle of the UAV, respectively; p_{ai} , q_{ai} , and r_{ai} are the angular velocities of the UAV rotating around the X_{ib} , Y_{ib} , and Z_{ib} axes, respectively.

2 Path error dynamics

According to Eq. (1), the kinematic model of the i -th USV can be expressed as

$$\begin{cases} \dot{x}_{si} = U_{si} \cos \psi_{siW} \\ \dot{y}_{si} = U_{si} \sin \psi_{siW} \\ \dot{\psi}_{siW} = r_{si} + \beta_{sid} \end{cases} \quad (3)$$

where $U_{si} = \sqrt{u_{si}^2 + v_{si}^2} > 0$ and is the actual speed of the USV; $\psi_{siW} = \psi_{si} + \beta_{si}$ and is the actual yaw angle of the USV. $\beta_{si} = \text{atan2}(v_{si}/u_{si})$ and is the sideslip angle of the USV, and $\beta_{sid} = \dot{\beta}_{si}$.

The parameterized path of the i -th USV can be expressed as $(x_{sid}(\chi_{si}), y_{sid}(\chi_{si}))$, where x_{sid} and y_{sid} are the positions of the waypoint in the fixed coordinate system $\{I\}$; χ_{si} is the path parameter of the i -th USV. Then, the tangent angle ψ_{sid} of a given path parameter of the USV can be denoted as

$$\psi_{sid} = \text{atan2}(y'_{sid}, x'_{sid}) \quad (4)$$

where $x'_{sid} = \partial x_{sid}(\chi_{si}) / \partial \chi_{si}$; $y'_{sid} = \partial y_{sid}(\chi_{si}) / \partial \chi_{si}$.

Concerning the i -th USV in position (x_{si}, y_{si}) , its longitudinal path-following error x_{sie} and transverse path-following error y_{sie} in the coordinate system tangential to the path can be expressed as

$$\begin{bmatrix} x_{sie} \\ y_{sie} \end{bmatrix} = \begin{bmatrix} \cos \psi_{sid} & -\sin \psi_{sid} \\ \sin \psi_{sid} & \cos \psi_{sid} \end{bmatrix}^T \begin{bmatrix} x_{si} - x_{sid}(\chi_{si}) \\ y_{si} - y_{sid}(\chi_{si}) \end{bmatrix} \quad (5)$$

The following equation can be obtained by taking the derivative of Eq. (5) and substituting Eq. (3)

$$\begin{cases} \dot{x}_{sie} = U_{si} \cos(\psi_{siW} - \psi_{sid}) + \dot{\psi}_{sid} y_{sie} - U_{sid} \dot{\chi}_{si} \\ \dot{y}_{sie} = U_{si} \sin(\psi_{siW} - \psi_{sid}) - \dot{\psi}_{sid} x_{sie} \end{cases} \quad (6)$$

where $U_{sid}^* = \sqrt{x_{sid}^2 + y_{sid}^2}$ and is the velocity of the i -th USV at the virtual reference point on the parameterized path.

For UAVs, a fluid coordinate system $\{A_i\}$ $O_{ib}X_{ia}Y_{ia}Z_{ia}$ as shown in Fig. 2 was built in this paper to design a 3D path-following controller suitable for motion control. The total velocity of the UAV in this coordinate system can be expressed as $U_{ai} = \sqrt{u_{ai}^2 + v_{ai}^2 + w_{ai}^2}$. Then, the angle of attack and sideslip angle of the UAV are $\alpha_{ai} = \arctan(w_{ai}/u_{ai})$ and $\beta_{ai} = \arcsin(v_{ai}/u_{ai})$, respectively, where $u_{ai} > 0$.

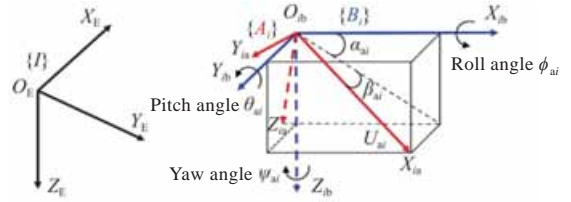


Fig. 2 3D coordinate system for motion control

Therefore, if the effect of the roll angle is ignored, the kinematic model of the i -th UAV can be expressed as

$$\begin{cases} \dot{x}_{ai} = U_{ai} \cos \Psi_{ai} \cos \Theta_{ai} \\ \dot{y}_{ai} = U_{ai} \sin \Psi_{ai} \cos \Theta_{ai} \\ \dot{z}_{ai} = -U_{ai} \sin \Theta_{ai} \\ \dot{\Theta}_{ai} = q_{ai} - \dot{\alpha}_{ai} \\ \dot{\Psi}_{ai} = \frac{r_{ai}}{\cos \theta_{ai}} + \dot{\beta}_{ai} \end{cases} \quad (7)$$

where Θ_{ai} and Ψ_{ai} are the track angle and azimuth angle of the i -th UAV, respectively.

A Serret-Frenet coordinate system $\{F_i\}$ $P_{ip}X_{ip}Y_{ip}Z_{ip}$ was constructed (Fig. 3), with an origin of P_{ip} and an update speed \dot{P}_{ip} of the path parameter. The parameterized path of the i -th UAV is expressed as $P_{aid}(\chi_{ai}) = (x_{aid}(\chi_{ai}), y_{aid}(\chi_{ai}), z_{aid}(\chi_{ai}))$, where x_{aid} , y_{aid} , and z_{aid} are the positions of the waypoint in the fixed coordinate system $\{I\}$; χ_{ai} is the path parameter of the i -th UAV. Then, the tangent angle of the path is

$$\begin{cases} \theta_{aid}(\chi_{ai}) = \arctan\left(\frac{-z'_{aid}(\chi_{ai})}{\sqrt{x_{aid}^2(\chi_{ai}) + y_{aid}^2(\chi_{ai})}}\right) \\ \psi_{aid}(\chi_{ai}) = \arctan\left(\frac{y'_{aid}(\chi_{ai})}{x'_{aid}(\chi_{ai})}\right) \end{cases} \quad (8)$$

where $x'_{aid}(\chi_{ai}) = \partial x_{aid} / \partial \chi_{ai}$; $y'_{aid}(\chi_{ai}) = \partial y_{aid} / \partial \chi_{ai}$; $z'_{aid}(\chi_{ai}) = \partial z_{aid} / \partial \chi_{ai}$.

In Fig. 3, for the i -th UAV in position (x_{ai}, y_{ai}, z_{ai}) , x_{aie} , y_{aie} , and z_{aie} are the longitudinal, transverse, and vertical path-following errors in the coordinate

system tangential to the path, respectively; $\theta_{ai eF} = \arctan(z_{ai e} / l_{ai})$, where l_{ai} is the lookahead distance; $\psi_{ai eF} = \arctan(-y_{ai} / l_{ai})$.

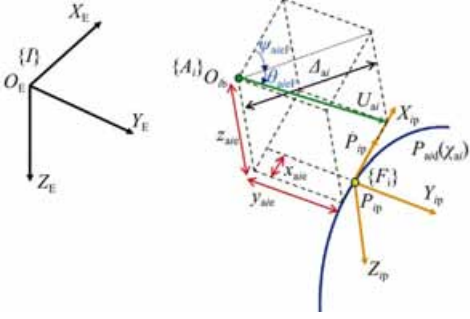


Fig. 3 3D reference coordinate system

The rotation matrix from the coordinate system $\{F_i\}$ to the coordinate system $\{I\}$ was defined as R_{Fai}^I . Then, it can be expressed as [20]

$$R_{Fai}^I = \begin{pmatrix} \cos \theta_{aid} \cos \psi_{aid} & -\sin \psi_{aid} & \sin \theta_{aid} \cos \psi_{aid} \\ \cos \theta_{aid} \sin \psi_{aid} & \cos \psi_{aid} & \sin \theta_{aid} \sin \psi_{aid} \\ -\sin \theta_{aid} & 0 & \cos \theta_{aid} \end{pmatrix} \quad (9)$$

The cooperative path-following error $\boldsymbol{\varepsilon}_{ai} = [x_{ai e}, y_{ai e}, z_{ai e}]^T$ can be rewritten as

$$\boldsymbol{\varepsilon}_{ai} = \mathbf{R}_{Fai}^{IT} (\boldsymbol{\eta}_{ai} - \boldsymbol{\eta}_{aid}) \quad (10)$$

where \mathbf{R}_{Fai}^{IT} is the transpose of the rotation matrix R_{Fai}^I ; $\boldsymbol{\eta}_{ai} = [x_{ai}, y_{ai}, z_{ai}]^T$ and is the actual position of the UAV; $\boldsymbol{\eta}_{aid} = [x_{ai}(\chi_{ai}), y_{ai}(\chi_{ai}), z_{ai}(\chi_{ai})]^T$ and is the position of the virtual reference point on a given path.

The following equation is obtained by taking the derivative of $\boldsymbol{\varepsilon}_{ai}$

$$\dot{\boldsymbol{\varepsilon}}_{ai} = \dot{\mathbf{R}}_{Fai}^{IT} (\boldsymbol{\eta}_{ai} - \boldsymbol{\eta}_{aid}) + \mathbf{R}_{Fai}^{IT} (\dot{\boldsymbol{\eta}}_{ai} - \dot{\boldsymbol{\eta}}_{aid}) \quad (11)$$

where $\dot{\mathbf{R}}_{Fai}^I = \mathbf{R}_{Fai}^I \mathbf{S}_{Fai}$.

Thereinto,

$$\mathbf{S}_{Fai} = \begin{bmatrix} 0 & -\dot{\psi}_{aid} \cos \theta_{aid} & \dot{\theta}_{aid} \\ \dot{\psi}_{aid} \cos \theta_{aid} & 0 & \dot{\psi}_{aid} \sin \theta_{aid} \\ -\dot{\theta}_{aid} & -\dot{\psi}_{aid} \sin \theta_{aid} & 0 \end{bmatrix} \quad (12)$$

The rotation matrix from the coordinate system $\{A_i\}$ to the coordinate system $\{F_i\}$ was defined as R_{AaiF}^F , and it could then be expressed as

$$R_{AaiF}^F = \begin{bmatrix} \cos \theta_{ai eF} \cos \psi_{ai eF} & -\sin \psi_{ai eF} & \sin \theta_{ai eF} \cos \psi_{ai eF} \\ \cos \theta_{ai eF} \sin \psi_{ai eF} & \cos \psi_{ai eF} & \sin \theta_{ai eF} \sin \psi_{ai eF} \\ -\sin \theta_{ai eF} & 0 & \cos \theta_{ai eF} \end{bmatrix} \quad (13)$$

The velocity of the i -th UAV in the fluid coordinate system $\{A_i\}$ was set as $\mathbf{U}_{aiA} = [U_{ai}, 0, 0]^T$, then

$$\dot{\boldsymbol{\eta}}_{ai} = \mathbf{R}_{Fai}^I \mathbf{R}_{AaiF}^F \mathbf{U}_{aiA} \quad (14)$$

Eq. (14) can be substituted into Eq. (11) to obtain

$$\begin{aligned} \dot{\boldsymbol{\varepsilon}}_{ai} &= \mathbf{S}_{Fai}^T \mathbf{R}_{Fai}^{IT} (\boldsymbol{\eta}_{ai} - \boldsymbol{\eta}_{aid}) + \mathbf{R}_{Fai}^{IT} (\dot{\boldsymbol{\eta}}_{ai} - \dot{\boldsymbol{\eta}}_{aid}) \\ &= \mathbf{S}_{Fai}^T \boldsymbol{\varepsilon}_{ai} + \mathbf{R}_{Fai}^{IT} \mathbf{U}_{aiA} - \mathbf{R}_{Fai}^{IT} \dot{\boldsymbol{\eta}}_{aid} \end{aligned} \quad (15)$$

Then, the path-following errors of the UAV can be expressed as

$$\begin{cases} \dot{x}_{ai e} = U_{ai} \cos \psi_{ai eF} \cos \theta_{ai eF} + \dot{\psi}_{aid} \cos \theta_{aid} y_{ai e} - \\ \quad \dot{\theta}_{aid} z_{ai e} - U_{aid}^* \dot{\chi}_{ai} \\ \dot{y}_{ai e} = U_{ai} \sin \psi_{ai eF} \cos \theta_{ai eF} - \dot{\psi}_{aid} \cos \theta_{aid} x_{ai e} - \\ \quad \dot{\psi}_{aid} \sin \theta_{aid} z_{ai e} \\ \dot{z}_{ai e} = -U_{ai} \sin \theta_{ai eF} + \dot{\theta}_{aid} x_{ai e} + \dot{\psi}_{aid} \sin \theta_{aid} y_{ai e} \end{cases} \quad (16)$$

where $U_{aid}^* = \sqrt{x_{aid}^2 + y_{aid}^2 + z_{aid}^2}$ and is the velocity of the i -th UAV at the virtual reference point on the parameterized path.

The control objective of this paper was to design a cooperative path-following controller for the UAVs and USVs so that they could follow the given parameterized path. Specifically, the control objective can be decomposed into the following two tasks:

1) The path-following task: the USVs and UAVs should be able to follow the given parameterized path, i.e.,

$$\lim_{t \rightarrow \infty} |x_{ie}| \rightarrow 0, \lim_{t \rightarrow \infty} |y_{ie}| \rightarrow 0, \lim_{t \rightarrow \infty} |z_{ie}| \rightarrow 0 \quad (17)$$

where t is time; $x_{ie} \in \{x_{s1e}, x_{s2e}, \dots, x_{sMe}, x_{a(M+1)e}, \dots, x_{aN e}\}$; $y_{ie} \in \{y_{s1e}, y_{s2e}, \dots, y_{sMe}, y_{a(M+1)e}, \dots, y_{aN e}\}$; $z_{ie} \in \{z_{a(M+1)e}, z_{a(M+2)e}, \dots, z_{aN e}\}$.

2) The path parameter cooperation task: for the system composed of UAVs and USVs, the path parameter of a given path should meet

$$\lim_{t \rightarrow \infty} |\chi_i - \chi_j| \rightarrow 0 \quad (18)$$

where $i = 1, 2, \dots, N$, and $j = 1, 2, \dots, N, i \neq j$, are the serial numbers of vehicles. When $i, j \in \{1, 2, \dots, M\}$, $(\chi_i, \chi_j) = (\chi_{si}, \chi_{sj})$; when $i, j \in \{M+1, M+2, \dots, N\}$, $(\chi_i, \chi_j) = (\chi_{ai}, \chi_{aj})$.

3 Controller design

3.1 Design of 3D LOS guidance law

When designing the guidance law of vehicles, this paper only investigated their kinematics. Therefore, an assumption was made as needed that both the UAVs and USVs could track the guidance signals provided by the kinematics as desired.

The 3D kinematic control law of UAVs was defined, and it was defined as follows

$$\begin{cases} \dot{\theta}_{ai e} = \theta_{ai} - \alpha_{ai} - \theta_{ai \theta} \\ \dot{\psi}_{ai e} = \psi_{ai} + \beta_{ai} - \psi_{ai \psi} \\ \dot{\chi}_{ai} = v_a - \omega_{ai} \end{cases} \quad (19)$$

where $\theta_{ai e}$ and $\psi_{ai e}$ are the track angle deviation and azimuth angle deviation of the i -th UAV, respectively; $\theta_{ai \theta} = \theta_{aid} + \theta_{ai eF}$ and $\psi_{ai \psi} = \psi_{aid} + \psi_{ai eF}$ are the guidance track angle and guidance azimuth angle of the i -th UAV, respectively; $\theta_{ai} \in (-\pi/2, \pi/2)$; v_a is the constant reference velocity of the UAV; ω_{ai} is the subsequent design variable for the i -th UAV.

According to Eq. (19), the Eq. (16) of the path-

following errors of the UAV can be rewritten as

$$\begin{cases} \dot{x}_{aie} = U_{ai} - U_{ai} \sin^2((\psi_{aieF} + \theta_{aieF})/2) + \dot{\psi}_{aid} \cos \theta_{aid} y_{aie} - \\ \quad U_{ai} \sin^2((\psi_{aieF} - \theta_{aieF})/2) - \dot{\theta}_{aid} z_{aie} - U_{aid}^* \dot{\chi}_{ai} \\ \dot{y}_{aie} = U_{ai} \sin \psi_{aieF} \cos \theta_{aieF} - \dot{\psi}_{aid} \cos \theta_{aid} x_{aie} - \\ \quad \dot{\psi}_{aid} \sin \theta_{aid} z_{aie} \\ \dot{z}_{aie} = -U_{ai} \sin \theta_{aieF} + \dot{\theta}_{aid} x_{aie} + \dot{\psi}_{aid} \sin \theta_{aid} y_{aie} \\ \dot{\Theta}_{aie} = q_{aiq} - \dot{\alpha}_{ai} - \dot{\Theta}_{ai\theta} \\ \dot{\Psi}_{aie} = r_{air} / \cos \theta_{ai} + \beta_{ai} - \dot{\Psi}_{ai\psi} \end{cases} \quad (20)$$

where q_{aiq} and r_{air} are the guidance pitch angular velocity and guidance yaw angular velocity of the i -th UAV, respectively.

The 3D LOS guidance law of the i -th UAV was defined as

$$\begin{cases} U_{aiU} = -k_{ai1} x_{aie} / \Pi_{aix} + U_{ai} \sin^2((\psi_{aieF} + \theta_{aieF})/2) + \\ \quad U_{ai} \sin^2((\psi_{aieF} - \theta_{aieF})/2) + U_{aid}^* v_a \\ \Theta_{ai\theta} = \theta_{aid} + \theta_{aieF} \\ \Psi_{ai\psi} = \psi_{aid} + \psi_{aieF} \\ q_{aiq} = -k_{ai2} \Theta_{aie} / \Pi_{ai\theta} + \dot{\alpha}_{ai} + \dot{\Theta}_{ai\theta} \\ r_{air} = -k_{ai3} \Psi_{aie} \cos \theta_{ai} / \Pi_{ai\psi} - (\dot{\beta}_{ai} - \dot{\Psi}_{ai\psi}) \cos \theta_{ai} \end{cases} \quad (21)$$

In the equation, U_{aiU} is the guidance velocity of the i -th UAV; $\Pi_{aix} = \sqrt{x_{aie}^2 + c_{aix}^2}$, $\Pi_{ai\theta} = \sqrt{\Theta_{aie}^2 + c_{ai\theta}^2}$, $\Pi_{ai\psi} = \sqrt{\Psi_{aie}^2 + c_{ai\psi}^2}$, where c_{aix} , $c_{ai\theta}$, and $c_{ai\psi}$ are all positive constants; k_{ai1} , k_{ai2} , and k_{ai3} are all positive constants as well.

Eq. (21) can be substituted into Eq. (20) to obtain

$$\begin{cases} \dot{x}_{aie} = -k_{ai1} x_{aie} / \Pi_{aix} + U_{aid}^* \omega_i + \dot{\psi}_{aid} \cos \theta_{aid} y_{aie} - \dot{\theta}_{aid} z_{aie} \\ \dot{y}_{aie} = -U_{ai} \cos \theta_{aieF} y_{aie} / \Pi_{aiy} - \dot{\psi}_{aid} \cos \theta_{aid} x_{aie} - \\ \quad \dot{\psi}_{aid} \sin \theta_{aid} z_{aie} \\ \dot{z}_{aie} = -U_{ai} z_{aie} / \Pi_{aiz} + \dot{\theta}_{aid} x_{aie} + \dot{\psi}_{aid} \sin \theta_{aid} y_{aie} \\ \dot{\Theta}_{aie} = -k_{ai2} \Theta_{aie} / \Pi_{ai\theta} \\ \dot{\Psi}_{aie} = -k_{ai3} \Psi_{aie} / \Pi_{ai\psi} \end{cases} \quad (22)$$

In the equation, $\Pi_{aiy} = \sqrt{y_{aie}^2 + c_{aiy}^2}$, $\Pi_{aiz} = \sqrt{z_{aie}^2 + c_{aiz}^2}$ where c_{aiy} and c_{aiz} are two positive constants.

Then, only the 2D horizontal plane was considered on the basis of the above 3D LOS guidance law to design the kinematic control law of the USV, and the law was defined as follows

$$\begin{cases} \Psi_{sie} = \psi_{siW} - \psi_{sir} \\ \dot{\chi}_{si} = v_s - \omega_{si} \end{cases} \quad (23)$$

In the equation, Ψ_{sie} is the yaw angle deviation of the i -th USV; ψ_{siW} and ψ_{sir} are the actual yaw angle and guidance yaw angle of the i -th USV, respectively; v_s is the constant reference speed of the USV; ω_{si} is the subsequent design variable for the i -th USV.

According to Eq. (23), the path-following errors

of the USV, namely Eq. (6), can be rewritten as

$$\begin{cases} \dot{x}_{sie} = U_{si} - 2U_{si} \sin^2\left(\frac{\psi_{siW} - \psi_{sid}}{2}\right) + \dot{\psi}_{sid} y_{sie} - U_{sid}^* (v_s - \omega_{si}) \\ \dot{y}_{sie} = U_{si} \sin(\psi_{sir} - \psi_{sid}) + \varrho_{si} - \dot{\psi}_{sid} x_{sie} \\ \dot{\Psi}_{sie} = r_{si} + \beta_{sid} - \dot{\psi}_{sir} \end{cases} \quad (24)$$

where $\varrho_{si} = U_{si} \sin(\psi_{siW} - \psi_{sid}) - U_{si} \sin(\psi_{sir} - \psi_{sid})$.

The LOS guidance law of the i -th USV was defined as

$$\begin{cases} U_{sir} = -k_{si4} x_{sie} / \Pi_{six} + U_{sid}^* v_s + 2U_{si} \sin^2\left(\frac{\psi_{siW} - \psi_{sid}}{2}\right) \\ r_{sir} = -k_{si5} \Psi_{sie} / \Pi_{si\psi} - \beta_{sid} + \dot{\psi}_{sir} - y_{sie} \varrho_{si} / \Psi_{sie} \end{cases} \quad (25)$$

In the equation,

$$\psi_{sir} = \psi_{sid} + \arctan\left(-\frac{y_{sie}}{l_{si}}\right) \quad (26)$$

where U_{sir} and r_{sir} are the guidance velocity and guidance angular velocity of the i -th USV, respectively; $\Pi_{six} = \sqrt{x_{sie}^2 + c_{six}^2}$; $\Pi_{si\psi} = \sqrt{\Psi_{sie}^2 + c_{si\psi}^2}$; l_{si} is the lookahead distance; c_{six} , $c_{si\psi}$, k_{si4} , and k_{si5} are all positive constants.

Eq. (25) can be substituted into Eq. (24) to obtain

$$\begin{cases} \dot{x}_{sie} = -k_{si4} x_{sie} / \Pi_{six} + U_{sid}^* \omega_{si} + \dot{\psi}_{sid} y_{sie} \\ \dot{y}_{sie} = -U_{si} y_{sie} / \Pi_{siy} + \varrho_{si} - \dot{\psi}_{sid} x_{sie} \\ \dot{\Psi}_{sie} = -k_{si5} \Psi_{sie} / \Pi_{si\psi} - y_{sie} \varrho_{si} / \Psi_{sie} \end{cases} \quad (27)$$

In this equation, $\Pi_{siy} = \sqrt{y_{sie}^2 + c_{siy}^2}$ where c_{siy} is the positive constant.

3.2 Design of path update rate

When a cooperative formation of multiple vehicles is examined, the communication topology graph \mathcal{G} among the vehicles can be represented by $\mathcal{G} = \{\mathcal{V}, \mathcal{E}\}$, where $\mathcal{V} = \{n_1, \dots, n_i, \dots, n_N\}$ is the node set and each vehicle corresponds to a node n_i ; $\mathcal{E} = \{(n_i, n_j) \in \mathcal{V} \times \mathcal{V}\}$ is the edge set. The adjacency matrix of the graph \mathcal{G} is $A = [a_{ij}]$. When $(n_i, n_j) \in \mathcal{E}$, $a_{ij} = 1$; otherwise, $a_{ij} = 0$. The matrix composed of the number of edges associated with the node n_i in the graph \mathcal{G} is the degree matrix D . Then, the Laplacian matrix of the graph \mathcal{G} can be expressed as $L = D - A$.

A definition was made that $\omega_i = \omega_{si}$ when $i \in \{1, 2, \dots, M\}$ and $\omega_i = \omega_{ai}$ when $i \in \{M+1, M+2, \dots, N\}$. In this section, the path parameters of the UAVs and USVs would be synchronized by designing ω_i to achieve the purpose of synchronous formation.

With the information on the neighboring UAVs or USVs, collaborative error e_i can be defined as

$$e_i = \sum_{j=1}^N a_{ij} (\chi_i - \chi_j) \quad (28)$$

where $i = 1, 2, \dots, N, j = 1, 2, \dots, N$, and $i \neq j$. $(\chi_i, \chi_j) = (\chi_{si}, \chi_{sj})$ when $i, j \in \{1, 2, \dots, M\}$, while $(\chi_i, \chi_j) = (\chi_{ai}, \chi_{aj})$ when $i, j \in \{M+1, M+2, \dots, N\}$. The matrix form of Eq. (28) can be expressed as $\mathbf{e} = \mathbf{L}\boldsymbol{\chi}$, where $\mathbf{e} = [e_1, e_2, \dots, e_N]^T$ and $\boldsymbol{\chi} = [\chi_1, \chi_2, \dots, \chi_N]^T$.

ω_i can be defined as

$$\omega_i = \mu_i e_i - \mu_i U_{id}^* x_{ie} \quad (29)$$

where μ_i is a positive constant; $i \in \{1, 2, \dots, M, M+1, \dots, N\}$. When $i \in \{1, 2, \dots, M\}$, $U_{id}^* = U_{sid}^*$, $x_{ie} = x_{sie}$, and $\omega_{ie} = \omega_{sie}$; when $i \in \{M+1, M+2, \dots, N\}$, $U_{id}^* = U_{aid}^*$, $x_{ie} = x_{aie}$, and $\omega_{ie} = \omega_{aie}$.

According to the graph theory [21], the error dynamic equation of the system composed of USVs and UAVs is

$$\begin{cases} \dot{x}_{sie} = -k_{si4} x_{sie} / \Pi_{six} + U_{sid}^* \omega_{si} + \dot{\psi}_{sid} y_{sie} \\ \dot{y}_{sie} = -U_{si} y_{sie} / \Pi_{siy} + \rho_{si} - \dot{\psi}_{sid} x_{sie} \\ \dot{\psi}_{sie} = -k_{si5} \Psi_{sie} / \Pi_{si\psi} - y_{sie} \rho_{si} / \Psi_{sie} \\ \dot{x}_{aie} = -k_{ai1} x_{aie} / \Pi_{aix} + U_{aid}^* \omega_i + \dot{\psi}_{aid} \cos \theta_{aid} y_{aie} - \dot{\theta}_{aid} z_{aie} \\ \dot{y}_{aie} = -U_{ai} \cos \theta_{aie} y_{aie} / \Pi_{aiy} - \dot{\psi}_{aid} \cos \theta_{aid} x_{aie} - \dot{\psi}_{aid} \sin \theta_{aid} z_{aie} \\ \dot{z}_{aie} = -U_{ai} z_{aie} / \Pi_{aiz} + \dot{\theta}_{aid} x_{aie} + \dot{\psi}_{aid} \sin \theta_{aid} y_{aie} \\ \dot{\theta}_{aie} = -k_{ai2} \Theta_{aie} / \Pi_{ai\theta} \\ \dot{\Psi}_{aie} = -k_{ai3} \Psi_{aie} / \Pi_{ai\psi} \\ \dot{e}_i = -\mathbf{L}\omega_i \end{cases} \quad (30)$$

where $i \in [1, M]$ in the subscript si ; $i \in [M+1, N]$ in the subscript ai .

4 Stability analysis

Lemma 1 [21]: If the graph \mathcal{G} is bidirectionally connected, a positive definite matrix \mathbf{P} exists such that $\boldsymbol{\chi}^T \mathbf{L}\boldsymbol{\chi} = \mathbf{e}^T \mathbf{P}\mathbf{e}$, where $\boldsymbol{\chi} = [\chi_1, \chi_2, \dots, \chi_N]^T$ and $\mathbf{e} = [e_1, e_2, \dots, e_N]^T$.

Lemma 2 [21]: If the graph \mathcal{G} is a balanced weakly connected graph, its Laplacian matrix \mathbf{L} should satisfy the following conditions.

1) The matrix $\text{Sym}(\mathbf{L}) = \frac{\mathbf{L} + \mathbf{L}^T}{2}$ is positive semi-definite.

2) If λ^* is defined as the minimum non-zero eigenvalue of the matrix $\text{Sym}(\mathbf{L})$, $\boldsymbol{\chi}^T \text{Sym}(\mathbf{L})\boldsymbol{\chi} \geq \lambda^* \left\| \boldsymbol{\chi} - \frac{\mathbf{1}_N \mathbf{1}_N^T}{N} \boldsymbol{\chi} \right\|^2$ holds for any $\boldsymbol{\chi} = [\chi_1, \chi_2, \dots, \chi_N]^T$, where $\mathbf{1}_N$ is an N -dimensional column vector with elements of one.

In the following, the stability of Eq. (30) of a closed-loop system would be proved by Theorem 1.

Theorem 1: On the basis of the motion equation of the USV, namely, Eq. (1), and that of the UAV, namely, Eq. (2), the guidance law of the USV, namely, Eq. (25), that of the UAV, namely, Eq. (21), and the cooperative update rate, namely, Eq. (29),

support that the origin of Eq. (30) of the closed-loop system satisfies $(x_{sie}, y_{sie}, \Psi_{sie}, x_{aie}, y_{aie}, z_{aie}, \Psi_{aie}, \Theta_{aie}, e_i) = (0, 0, 0, 0, 0, 0, 0, 0, 0)$ under the condition that the USVs and UAVs can follow the given guidance velocity and guidance angular velocity as desired. This is globally uniformly asymptotically stable.

Proof: A Lyapunov function V_1 was constructed

$$V_1 = \frac{1}{2} \sum_{i=1}^M \{x_{sie}^2 + y_{sie}^2 + \Psi_{sie}^2\} + \frac{1}{2} \sum_{i=M+1}^N \{x_{aie}^2 + y_{aie}^2 + z_{aie}^2 + \Theta_{aie}^2 + \Psi_{aie}^2\} + \boldsymbol{\chi}^T \mathbf{L}\boldsymbol{\chi} \quad (31)$$

According to Lemma 1, V_1 can be rewritten as

$$V_1 = \frac{1}{2} \sum_{i=1}^M \{x_{sie}^2 + y_{sie}^2 + \Psi_{sie}^2\} + \frac{1}{2} \sum_{i=M+1}^N \{x_{aie}^2 + y_{aie}^2 + z_{aie}^2 + \Theta_{aie}^2 + \Psi_{aie}^2\} + \mathbf{e}^T \mathbf{P}\mathbf{e} \quad (32)$$

The following equation can be obtained by taking the derivative of Eq. (32) and substituting Eq. (30)

$$\begin{aligned} \dot{V}_1 \leq & \sum_{i=1}^M \left\{ -\frac{k_{si4} x_{sie}^2}{\Pi_{six}} + U_{sid}^* \omega_i x_{sie} - \frac{U_{si} y_{sie}^2}{\Pi_{siy}} - \frac{k_{si5} \Psi_{sie}^2}{\Pi_{si\psi}} \right\} + \\ & \sum_{i=M+1}^N \left\{ -\frac{k_{ai1} x_{aie}^2}{\Pi_{aix}} - \frac{U_{ai} \cos \theta_{aie} y_{aie}^2}{\Pi_{aiy}} - \frac{U_{ai} z_{aie}^2}{\Pi_{aiz}} - \right. \\ & \left. \frac{k_{ai2} \Theta_{aie}^2}{\Pi_{ai\theta}} - \frac{k_{ai3} \Psi_{aie}^2}{\Pi_{ai\psi}} + U_{aid}^* \omega_i x_{aie} \right\} - \boldsymbol{\chi}^T \mathbf{L}\boldsymbol{\omega} \leq \\ & \sum_{i=1}^M \left\{ -\frac{k_{si4} x_{sie}^2}{\Pi_{six}} - \frac{U_{si} y_{sie}^2}{\Pi_{siy}} - \frac{k_{si5} \Psi_{sie}^2}{\Pi_{si\psi}} \right\} + \\ & \sum_{i=M+1}^N \left\{ -\frac{k_{ai1} x_{aie}^2}{\Pi_{aix}} - \frac{U_{ai} \cos \theta_{aie} y_{aie}^2}{\Pi_{aiy}} - \frac{U_{ai} z_{aie}^2}{\Pi_{aiz}} - \right. \\ & \left. \frac{k_{ai2} \Theta_{aie}^2}{\Pi_{ai\theta}} - \frac{k_{ai3} \Psi_{aie}^2}{\Pi_{ai\psi}} \right\} - \lambda_{\min}(\boldsymbol{\mu}) \|\boldsymbol{\theta}\|^2 \quad (33) \end{aligned}$$

In the equation, $\boldsymbol{\omega} = [\omega_{s1d}, \omega_{s2d}, \dots, \omega_{sMd}, \omega_{a(M+1)d}, \dots, \omega_{aNd}]^T$; $\lambda_{\min}(\boldsymbol{\mu})$ is the minimum eigenvalue of the matrix $\boldsymbol{\mu}$ and $\boldsymbol{\mu} = \text{diag}\{\mu_i\} = \text{diag}\{\mu_1, \mu_2, \dots, \mu_M, \mu_{M+1}, \dots, \mu_N\}$; $\boldsymbol{\theta} = -\mathbf{e} + \mathbf{U}_{id}^* \mathbf{x}_e$, in which $\mathbf{U}_{id}^* = \text{diag}\{U_{sid}^*, U_{s2d}^*, \dots, U_{sMd}^*, U_{a(M+1)d}^*, \dots, U_{aNd}^*\}$ and $\mathbf{x}_e = [x_{s1e}, x_{s2e}, \dots, x_{sMe}, x_{a(M+1)e}, \dots, x_{aNe}]^T$.

Theorem 2.1 in Ref. [22] can be referred to to prove that the origin of Eq. (30) of the closed-loop system is globally uniformly asymptotically stable.

According to Lemma 1 and Lemma 2,

$$\mathbf{e}^T \mathbf{P}\mathbf{e} \geq \lambda^* \left\| \boldsymbol{\chi} - \mathbf{1}_N \frac{1}{N} \sum_{i=1}^N \chi_i \right\|^2 \quad (34)$$

holds. Since e_i is bounded, $\chi_i \rightarrow \chi_j \rightarrow \frac{1}{N} \sum_{i=1}^N \chi_i$, namely that the cooperative path parameter control objective of Eq. (19) is achieved.

5 Numerical simulation

To verify the effectiveness of the proposed cooperative path-following control method for UAVs and USVs, this section simulates an unmanned cluster system composed of three USVs [23] and three UAVs [19].

The three UAVs took off from the corresponding USVs, respectively, and the six unmanned vehicles all adopted the path-following method to form a formation for cooperative search and rescue. The search area was a cuboid area. The design parameters of the controller were $k_{ai1} = 0.5$, $k_{ai2} = 0.3$, $k_{ai3} = 0.2$, $k_{si4} = 0.5$, and $k_{si5} = 0.2$. The initial positions of the three USVs were that $(x_1, y_1, z_1) = (-10, 18, 0)$, $(x_2, y_2, z_2) = (-11, 0, 0)$, and $(x_3, y_3, z_3) = (-12, 15, 0)$. Those of the three UAVs were that $(x_4, y_4, z_4) = (-10, 18, 0)$, $(x_5, y_5, z_5) = (-11, 0, 0)$, and $(x_6, y_6, z_6) = (-12, 15, 0)$.

Fig. 4 shows the cooperative path-following results of the heterogeneous unmanned system composed of the USVs and UAVs. From the figure, the three USVs (USV1, USV2, USV3) and the three UAVs (UAV1, UAV2, UAV3) can all track the preset parameterized path, where the blue dots represent the USVs and the green ones are the UAVs. Fig. 5 presents the path parameters of the system. According to the figure, the path parameters of the three USVs and those of the three UAVs tend to be consistent with each other after a period of time, indicating the fulfillment of the objective of parameter coordination. Figs. 6–8 illustrate the guidance velocity U_i ($U_i \in \{U_{s1r}, U_{s2r}, \dots, U_{sMr}, U_{a(M+1)U}, \dots, U_{aNu}\}$), guidance angular velocity q_i ($q_i \in \{q_{a(M+1)q}, q_{a(M+2)q}, \dots, q_{aNq}\}$), and guidance angular velocity r_i ($r_i \in \{r_{s1r}, r_{s2r}, \dots, r_{sMr}, r_{a(M+1)r}, \dots, r_{aNr}\}$) of the UAVs and USVs, respectively. These figures indicate that after the dynamic adjustment, the guidance velocity and guidance angular velocities of the system all tend to be consistent, representing synchro-

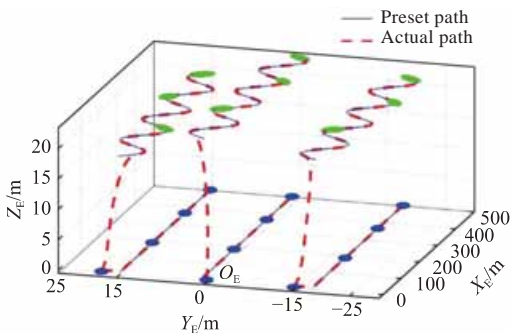


Fig. 4 Path-following performance

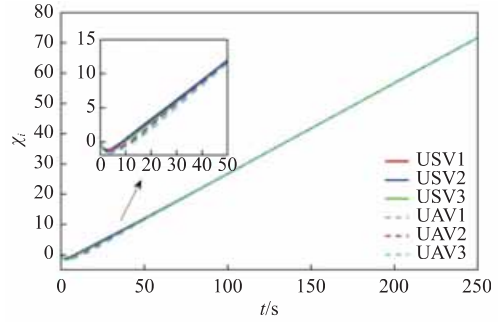


Fig. 5 Path parameter

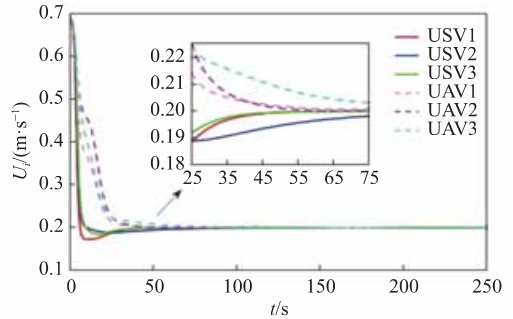


Fig. 6 Guidance velocity U_i

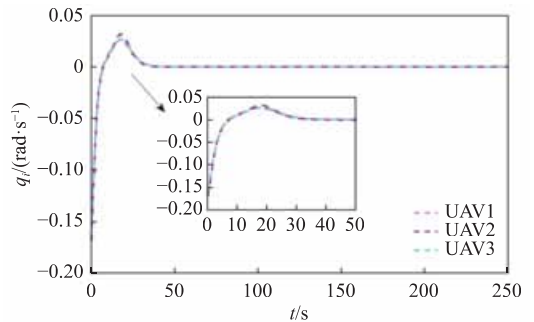


Fig. 7 Guidance angular velocity q_i

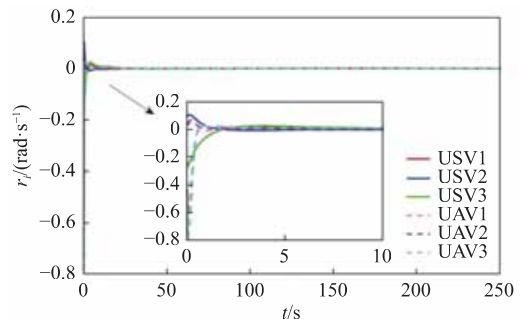
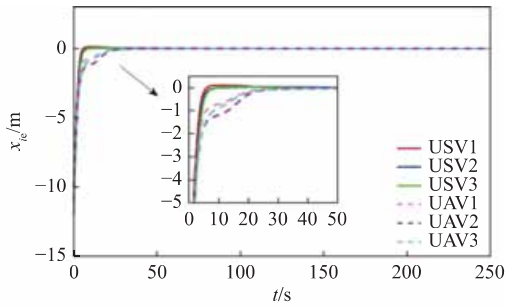
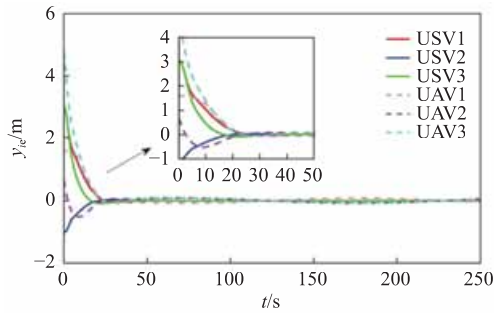
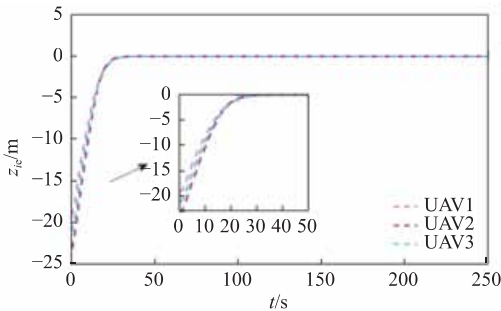


Fig. 8 Guidance angular velocity r_i

nous path-following. Figs. 9–11 show the cooperative path-following errors x_{ie} , y_{ie} , x_{ie} of the system, respectively. Clearly, the path-following errors approach zero after a period of time, which indicates that the cooperative path-following control method for heterogeneous marine vehicles proposed in this paper can well complete the cooperative control task.

Fig. 9 Cooperative path-following error x_{ie} Fig. 10 Cooperative path-following error y_{ie} Fig. 11 Cooperative path-following error z_{ie}

6 Conclusions

In this paper, an unmanned heterogeneous cluster system composed of UAVs and USVs was taken as the research object. Regarding the practical problem of the cooperative path-following control of the system for maritime search and rescue, the kinematic models of the UAVs and USVs were constructed by introducing a fixed coordinate system and a vehicle body coordinate system. Furthermore, a cooperative path-following control method for the heterogeneous marine vehicles was designed on the basis of 3D LOS guidance laws so that the unmanned cluster system composed of the UAVs and USVs could effectively follow the preset parameterized path. Finally, the stability of the proposed control system was analyzed by the Lyapunov stability theory. The simulation results demonstrate the effectiveness of the proposed 3D heterogeneous cooperative path-following controller for marine search and rescue. The following research work will further

discuss the problem of sea-air cooperative search and rescue based on time consistency and dynamic control.

References

- [1] ANG T T, JIANG Z, SUN R J, et al. Maritime search and rescue based on group mobile computing for unmanned aerial vehicles and unmanned surface vehicles [J]. *IEEE Transactions on Industrial Informatics*, 2020, 16(12): 7700–7708.
- [2] MACWAN A, VILELA J, NEJAT G, et al. A multi-robot path-planning strategy for autonomous wilderness search and rescue [J]. *IEEE Transactions on Cybernetics*, 2015, 45(9): 1784–1797.
- [3] XU X B, DUAN H B, ZENG Z G, et al. Progresses in UAV/USV cooperative control [J]. *Aero Weaponry*, 2020, 27(6): 1–6 (in Chinese).
- [4] LIU C G, CHU X M, MAO Q X, et al. Adaptive path following control system for unmanned surface vehicles [J]. *Journal of Mechanical Engineering*, 2020, 56(8): 216–227 (in Chinese).
- [5] LUAN T Y, ZHANG Y F, ZHANG C W, et al. Path following control of USV considering disturbance and model uncertainty [J]. *Computer Knowledge and Technology*, 2021, 17(9): 223–226, 233 (in Chinese).
- [6] YU Y L, SU R S, FENG X, et al. Tracking control of backstepping adaptive path of unmanned surface vessels based on surge-varying LOS [J]. *Chinese Journal of Ship Research*, 2019, 14(3): 163–171 (in Chinese).
- [7] GU N, PENG Z H, WANG D, et al. Antidisturbance coordinated path following control of robotic autonomous surface vehicles: theory and experiment [J]. *IEEE/ASME Transactions on Mechatronics*, 2019, 24(5): 2386–2396.
- [8] LIU L, WANG D, PENG Z H, et al. Cooperative path following ring-networked under-actuated autonomous surface vehicles: algorithms and experimental results [J]. *IEEE Transactions on Cybernetics*, 2020, 50(4): 1519–1529.
- [9] GU N, WANG D, PENG Z H, et al. Advances in line-of-sight guidance for path following of autonomous marine vehicles: an overview [J/OL]. *IEEE Transactions on Systems, Man, and Cybernetics: Systems*. <https://ieeexplore.ieee.org/document/9750396>.
- [10] ZHANG Y T, ZHANG Y M, LIU Z X, et al. Line-of-sight path following control on UAV with sideslip estimation and compensation [C]//*Proceedings of the 37th Chinese Control Conference (CCC)*. Wuhan, China: IEEE, 2018: 4711–4716.
- [11] GHOMMAM J, SAAD M. Coordinated 3D path following control for a team of UAVs with reference velocity recovery [C]//*Proceedings of 2009 European Control Conference (ECC)*. Budapest, Hungary: IEEE, 2009: 3008–3014.
- [12] JIN X, MEI W, YANG Z L. Path following control for unmanned aerial vehicle based on carrot chasing algo-

- rithm and PLOS [C] //Proceedings of 2020 IEEE International Conference on Artificial Intelligence and Information Systems (ICAIS). Dalian, China: IEEE, 2020: 571–576.
- [13] CUI Z Y, WANG Y. Fault-tolerant fixed-time path following guidance control of UAV [J]. Journal of Beijing University of Aeronautics and Astronautics, 2021, 47(8): 1619–1627 (in Chinese).
- [14] YAN Z Y, WANG D B, WANG B H, et al. 3D path tracking control of UAV based on vector field method [J]. Machinery & Electronics, 2021, 39(10): 50–56 (in Chinese).
- [15] LIU R H, LIU S G, ZHANG B Y, et al. 3D cooperative path following control of multi-UAVs with input saturation [J]. Journal of Beijing University of Aeronautics and Astronautics, 2022, 48(6): 1038 – 1049 (in Chinese).
- [16] PENG Z, WANG D, HU X. Robust adaptive formation control of underactuated autonomous surface vehicles with uncertain dynamics [J]. IET Control Theory & Applications, 2011, 5(12): 1378–1387.
- [17] FOSSEN T I. Marine control systems: guidance, navigation and control of ships, rigs and underwater vehicles [M]. Trondheim, Norway: Marine Cybernetics, 2002.
- [18] SCHIRRER A, WESTERMAYER C, HEMEDI M, et al. LQ-based design of the inner loop lateral control for a large flexible BWB-type aircraft [C]//Proceedings of 2010 IEEE International Conference on Control Applications. Yokohama, Japan: IEEE, 2010: 1850–1855.
- [19] SHI Z Y. Research on UAV 3D path planning and control algorithm [D]. Chengdu: University of Electronic Science and Technology of China, 2021 (in Chinese).
- [20] TANAKA K, TANAKA M, TAKAHASHI Y, et al. 3-D flight path tracking control for unmanned aerial vehicles under wind environments [J]. IEEE Transactions on Vehicular Technology, 2019, 68(12): 11621–11634.
- [21] CERAGIOLI F, DE PERSIS C, FRASCA P. Discontinuities and hysteresis in quantized average consensus [J]. Automatica, 2011, 47(9): 1916–1928.
- [22] KRSTIĆ M, KANELAKOPOULOS I, KOKOTOVIĆ P. Nonlinear and adaptive control design [M]. New York: John Wiley & Sons, 1995.
- [23] LIU L, WANG D, PENG Z H, et al. Distributed path following of multiple under-actuated autonomous surface vehicles based on data-driven neural predictors via integral concurrent learning [J]. IEEE Transactions on Neural Networks and Learning Systems, 2021, 32(12): 5334–5344.

面向海上搜救的 UAV 与 USV 集群 协同路径跟踪控制

王浩亮¹, 尹晨阳¹, 卢雨宇¹, 王丹², 彭周华^{*2}

1 大连海事大学 轮机工程学院, 辽宁 大连 116026

2 大连海事大学 船舶电气工程学院, 辽宁 大连 116026

摘要: [目的] 针对由无人机 (UAV) 与水面无人艇 (USV) 组成的异构无人集群系统, 研究其在海上搜救过程中的三维协同路径跟踪控制问题。 [方法] 首先, 在固定坐标系和机体坐标系下建立 UAV 和 USV 的运动学模型, 同时建立流体坐标系, 以设计适宜运动控制的三维路径跟踪控制器, 并在 Serret-Frenet 坐标系下建立 UAV 和 USV 的路径跟踪误差模型; 然后, 在运动学层面设计三维视线 (LOS) 制导律, 并基于此提出一种适用于异构海洋航行器集群的协同路径跟踪控制方法, 从而使 UAV 与 USV 组成的集群系统可以有效跟踪设定的参数化路径; 最后, 基于李雅普诺夫稳定性理论分析该控制系统的稳定性。 [结果] 仿真结果验证了所提异构海洋航行器集群协同路径跟踪控制方法的有效性。 [结论] 研究成果可为面向海上搜救的无人航行器集群协同路径跟踪控制方法提供参考。

关键词: 海上搜救; 无人机; 水面无人艇; 三维视线制导律; 协同路径跟踪